International Journal of Modern Engineering Research (IJMER)
www.ijmer.com Vol. 3, Issue. 6, Nov - Dec. 2013 pp-3305-3319 ISSN: 2249-6645

Energy Losses And Turbulence Characteristics Through Hydraulic Structures Using Laser Doppler Velocimetry(LDV)

M. I. Attia

Assoc. Prof., Water & Water Structures Engg. Dept. Faculty of Engg., Zagazig University, Zagazig,Egypt,

ABSTRACT: *This paper deals with the experimental investigation of energy losses and turbulence characteristics through hydraulic structures in a rectangular channel using Laser Doppler, measurements include turbulence intensity components and mean velocity components. Experiments were conducted with different contraction ratios at different expansion angles for different bed slopes. The results show that, the rate of variation of the energy loss increases till expansion angle about 30°. This rate of increase decreases above this value of angle of expansion. The energy loss is quite high at a contraction ratio of 0.7. Also, the results clearly show that, gradual expansion decrease the turbulence intensities in the wall and free surface regions compared to the sudden expansion. The maximum values of the turbulence intensities occur either close to the bed or at the free surface, with minimum values occurring within the core region. The turbulence intensities, however increases sharply at the free surface due to the free surface waves effect, and is the largest in sudden expansion.*

KEY WORDS: *Energy losses-Turbulence characteristics-Hydraulic structures-Laser Doppler velocimery-Contraction ratio-Free surface-Froude number-Expansion angle.*

I. INTRODUCTION

The information regarding the turbulence characteristics in the transitional structures is somewhat scanty. Paradoxically enough, the problem of separation of the main stream of flow at open channel transitions or at an abrupt change of the boundary attracted the attention of investigators since the earliest time and yet it remains one of the least understood and the most critical problems of fluid dynamics today. Open channel transitions are commonly used in hydraulic structures in variety of situation to serve as link with minimum possible energy loss. Open channel transitions have been studied extensively because of their use in water resources engineering and their efficacy in reducing the energy loss in hydraulic structures. Transitions are provided, whenever the size or the shape of the cross section of an open channel changes. Such changes are often required in natural and artificial channels for water structures economically as well as for practical reasons. The transitions may be vertical or horizontal, contracting or expanding, sudden or gradually which are required for subcritical or supercritical flows. The change in the cross section disturbs the flow in the contracted reach and near it from both upstream and downstream. The change in the cross section, slope, and/or alignment over a specified reach is termed local transition, such channel transition is used mainly to avoid or minimize the excessive energy loss, to eliminate the cross waves, the resulting turbulence and to ensure safety of both the structure and the downstream channel reach. In the design of hydraulic structures, designers do their best to avoid sudden transition of the flow by sudden contractions to ensure smooth flow with minimum energy loss and to reduce turbulence pattern. As the flow passes through a bridge, a channel transition in the form of contraction and subsequent expansion is involved. Since these transitions are meant for continuous use, their role in minimization of the energy loss and attenuation of turbulence assumes significance. It is indispensable in hydraulic engineering to investigate structures of turbulence behind of multi vents water structures in the expansion zone in order to control turbulent flows and to design hydraulic structures properly. In designing of channel transitions, it is necessary to avoid excessive energy loss, to eliminate cross waves and the turbulence, to ensure smooth streamlined flow, to minimize standing waves, and to prevent the transition from acting as a choke influencing upstream flow. Free surface has a unique role in governing the turbulence in open channel flows. The phenomenon is usually so complicated that the resulting flow pattern is not readily subjected to any analytical solution. So, a practical solution is possible, however, through experimental investigation. The turbulent flow models in open channel flows were discussed by Garde [5,6], Rodi [12]; Nezu [10]. Measurements of turbulence characteristics in open channel flows using LDA have been pointed by several investigators [7, 9, 13, 14]. Experimental investigation of turbulent structure of back facing step have been reported by several investigators. [1, 8, 11, 3]. The main results of Formica were reported in Chow [2]. The present study of the how characteristics and turbulence structure behind of multi vents water structures, is a typical case of separation at an abrupt change of boundary. Thus, one of the purposes to study the turbulence behind of water structures in the expansion zone is to gain in sight into the properties and interactions of these turbulent structures. Much less information is available regarding the turbulence characteristics in the expansion zone of water structures.

Therefore, precise and accurate measurements of the energy loss are carried out to study the variation of the energy loss upstream, within and downstream of the multi vents water structures. Also, the present research involves measurements of mean and fluctuating flow characteristics such as streamwise and vertical turbulence intensities, and streamwise and vertical mean velocity components in the expansion zone behind the multi vents water structures. The measurements are carried out using a Laser Doppler Velocimetry(LDV)a non-intrusive Fiber Optic state of the art technique, in the expansion zones of water structures at different contraction ratio b/B of 0.9, 0.8, 0.7, 0.6, 0.5 and 0.4 at different expansion angles θ of 15°, 30°, 45°, 60°, 75°, and 90° for various bottom slope S_o of 0.005, 0.01, 0.015, 0.02, and 0.025. Also, the objectives of the present research are: to use LDV, which includes the data acquisition system, data processing to measure mean and fluctuating flow characteristics at different locations in the expansion zones of the water structures; to conduct a comparative study of the depthwise variation of streamwise and vertical turbulence intensities at different cross sections in the expansion

zones of water structures, to make a comparative study of the depthwise variation of water structures, to make a comparative study of the depthwise variation of streamwise and vertical mean velocity components. Similarly, the measurements were made in the expansion zones along the centerline at relative depth ratio y/y_o of 0.5 to study the variation of mean and fluctuating flow characteristics.

II. THEORETICAL STUDY

In the flow over the water structure through a channel, part of pressure head will lost partly due to dissipation of energy in separation zones, and partly due to friction between fluid and the channel wetted parameter. On the other hand, the constriction of flow by contraction will result in a corresponding backwater build up. Figure.3 shows a definition sketch of flow through contraction in sloping channel. The variables affecting the flow through the multi vents water structure are shown on the figure and explained at the notation section. The functional relationship of the energy loss through the water structure could be written as follows:

$$f_1(g, V_u, Y_u, b, B, Y_d, V_d, \Delta E, \Delta E_u, \Delta E_d, S_o, \theta) = 0 \quad (1)$$

Using the dimensional analysis, the following dimensionless relationship is obtained:

$$\frac{\Delta E}{Y_u} = f_2\left[F_u, \frac{b}{Y_u}, \frac{B}{Y_u}, S_o, \theta\right] \quad (2)$$

Keeping in mind the properties on the non-dimensional quantities, the following expression could be obtained from Eq. (2)

$$\frac{\Delta E}{Y_u} = f_3\left[F_u, \frac{b}{B}, S_o, \theta\right] \quad (3)$$

It may appear better to analyze the energy loss through the water structures as a ratio related to the upstream energy, E_u. Therefore, the E_u is used instead of Y_u in the left hand side of equation (3) which becomes:

$$\frac{\Delta E}{E_u} = f_4\left[F_u, \frac{b}{B}, S_o, \theta\right] \quad (4)$$

The energy loss through the transition is equal to the difference in specific energies before and after the transition. From Fig.3, applying specific energy equation between sections (1-1) and (3-3)

$$\Delta E = E_u - E_d = \left(y_u + \frac{{V_u}^2}{2g}\right) - \left(y_d + \frac{{V_d}^2}{2g}\right) \quad (5)$$

And relative energy loss is expressed as

$$\frac{\Delta E}{E_u} = 1 - \frac{E_d}{E_u} \quad (6)$$

Similarly to equation (6), from Fig.3, applying the specific energy equation between sections (1-1) and (2-2) also between sections (2-2) and (3-3).

$$\frac{\Delta E_u}{E_u} = 1 - \frac{E_t}{E_u}, \text{and} \quad (7)$$

$$\frac{\Delta E_d}{E_d} = \frac{Et}{Ed} - 1 \quad (8)$$

Where;

E_u, E_t and E_d, specific energy upstream, within and downstream the water structure respectively, ΔE= total energy loss between sections (1-1) and (3-3), ΔE_u = upstream energy loss between sections (1-1) and (2-2), ΔE_d = downstream energy loss between sections (2-2) and (3-3).By knowing either the value of velocity or water depth upstream, within and downstream the multi water structure, the energy loss can be calculated by using equations (6), (7) and (8) for the known values of discharges and different contraction ratios b/B at different expansion angles θ.

III. EXPERIMENTAL SET UP AND PROCEDURE

The experiments were carried out in a rectangular open channel that is 8.0m long, 0.3m width and 0.5m height with glass wall 6 mm thick and a steel plate bed Fig.1 shows layout of the test facility. The water is supplied from a constant head overhead tank to the flume at a desired discharge that is continuously monitored with an on-line orifice meter. The discharges were measured using a pre-calibrated orifice meter in the feeding pipeline. And in-line discharge control valve that is fitted into the main supplying pipeline was used to regulate the flow rate. Depth measurements were taken using a needle point gauge with a reading accuracy of ± 0.10 mm. The flume side walls are made up of 6 mm glass sheets. A tail gate is provided at the downstream end of the flume to maintain a required water depth of the channel flow. The water is finally collected in a sump placed in the basement from where it is pumped back to the overhead tank by a 15 Hp pump. The experiments were carried out using six different lateral contraction ratios, b/B of 0.9, 0.8, 0.7, 0.6, 0.5, and 0.4 and five different expansion angles, θ of 15°, 30°, 45°, 60°, 75°, and 90°. Five different channel bottom positive slopes, S_o of 0.005, 0.01, 0.015, 0.02, and 0.025 were used to illustrate the effect of bottom slope on the flow characteristics due to contraction. The slopes were selected based on the flume facilities. For each combination of lateral contraction ratio, b/B, expansion angles, θ, and bottom slope, five different flow rates ranging from about 15 Lit/sec to 40 Lit/sec were used. The upstream water depth was adjusted to produce a Froude number of approach ranging from 0.10 to 0.4. The flow through the transition was always subcritical but it may changed to supercritical state just at the end of the transition or away from it, depending upon the incoming flow rate, the applied flume bottom slope, the expansion angle and the contraction ratio. The effect of the expansion angle θ on the energy loss and turbulence intensities was also studied, for a different lateral contraction ratios b/B and a different bottom slope S_o. Channel transitions were fabricated from transparent prespex sheets. One type of construction at the inlet was sudden and different expansions at the outlet were at expansion angles θ of 15°, 30°, 45°, 60°, 75°, and 90° downstream of two vents water structure.

IV. LASER DOPPLER TECHNIQUE

The experimental data were collected using the two color back scatter Laser Doppler Velocimetry (LDV) system. Fig.2 shows a block diagram of the two component LDV set up used for the measurements. A 5 Watt Argon-ion laser with two laser beams; one blue (488nm) and one green (514.5nm), were focused at a measuring point from one side of the channel through an optical lens. Two Burst Spectrum Analyzers (BSA) were used to evaluate the Doppler frequencies. Subsequent computer analysis consisted of velocity bias averaging and outlier rejection. The number of samples taken at every point was 5000 bursts. This correspond to a simple averaging time of about 100 seconds. The data rate was about (50-60) per second. Before acquiring the data, the LDV signal was checked for its quality on a 100 MHz Gold storage oscilloscope. The signal display as regular Doppler burst that correspond to a particle passing through the measuring volume. The measurements were taken at different cross sections in the expansion zones downstream of two vents water structure for different flow rate (Q). Fig.3 shows the location grid of the measuring stations.

With reference to the origin fixed at the channel bed and in the centre of lower vent as shown in Fig.3, transverse of measuring volume was run to obtain the profiles of both the RMS of the streamwise and vertical turbulence intensities, and streamwise and vertical mean velocity components. The measuring points were closely spaced in the region of high velocity gradient. All the measurements were made for a constant free steam water depth of 31cm irrespective of the flow rate. To obtain the vertical profiles of the mean and fluctuating flow quantities, the measurements were conducted in the vertical plane at z/b= 0 and 0.3 at different cross sections at different flow rates. In the vertical direction at every profile, 30 measurements at 5mm intervals up to 60 mm from the bed boundary and 15mm for the rest were taken. Similarly, the measurements were done in the expansion zones along the centerline at relative water depth y/y_o= 0.5 to study the variation of mean and fluctuating flow characteristics.

V. RESULTS AND DISCUSSION

The relative total energy loss with regard to the energy upstream of the multi water structure $\Delta E/E_u$ is plotted as a function of downstream expansion angles θ of 15°, 30°, 45°, 60°, 75°, and 90° at different contraction ratios b/B of 0.9, 0.8, 0.7, 0.6, 0.5 and 0.4 at various bottom slope S_o of 0.005, 0.01, 0.015, 0.02 and 0.025, Fig.4. The total energy loss is the least value for channel contraction b/B of 0.9 and a maximum value for channel contraction b/B of 0.4. It is relatively small up to the contraction ratio b/B of 0.7. The rate of increase in energy loss, Fig.4, is almost the same between the contraction ratios b/B of 0.9 and 0.8; and 0.8 and 0.7. By taking the value of the rate of increase in energy loss between contraction ratios b/B of 0.9 and 0.8; and 0.8 and 0.7 as a reference. This rate of increase in energy loss has the double value between the contraction ratios b/B of 0.7 and 0.6. Similarly, this rate of increase in energy loss increases to about (5-6) times between b/B of 0.6 and 0.5 and almost about (10-12) times between contraction ratios b/B of 0.5 and 0.4 as compared to the increase in energy loss between the contraction ratios b/B of 0.9 and 0.8. This trend is almost the same for all other contraction. As the expansion angle θ increases up to 30°, the rate of increase in the head loss $\Delta E/E_u$ is relatively high for all the contraction ratios b/B, being very high for the contraction ratio b/B of 0.6. Above expansion angle θ of 30°, the increase in the energy loss is much slower. Particularly for expansion angle θ greater than 45° at which the energy loss is almost constant for all the practical purposes. Also, as shown in Fig.4, the energy loss $\Delta E/E_u$ increases with the increase of bottom slope S_o.

Fig.5 depicts the variation of total relative energy loss $\Delta E/E_u$ with regard to the energy upstream with bottom slope S_o at different contraction ratios b/B of 0.9, 0.8, 0.7, 0.6, 0.5 and 0.4 at different expansion angles θ of 15°, 30°, 45°, and 90°. From this figure, it can be observed that for a fixed expansion angle θ, the trend of variation between relative energy loss $\Delta E/E_u$ and bottom slope S_o is increasing with a nonlinear trend. Also, at a particular bottom slope S_o, relative energy loss $\Delta E/E_u$ as the channel contraction b/B increases.

Fig.6 shows the variation of relative total energy loss $\Delta E/E_u$ with upstream Froude number F_u for different contraction ratios b/B of 0.9, 0.8, 0.7, 0.6, 0.5 and 0.4 for the flow rates Q of 15 Lit/sec and 40 Lit/sec. Several Froude numbers respect to upstream depth were generated from these discharges by changing the depths for the given discharges. It can be noticed from the figure that the relationship between F_u and $\Delta E/E_u$ is a family of curves. The nature of the trend of variation of total energy loss $\Delta E/E_u$ is similar in all cases of flow. The curves are extended backward from F_u=0.05 and 0.1 for comparative purpose. With an increasing Froude number F_u, the energy loss $\Delta E/E_u$ increases with a slightly slower rate up to F_u = 0.2 say, for contraction ratio b/B > 0.5 , the energy loss $\Delta E/E_u$ is small up to say F_u=0.1, after which energy loss increases rapidly as Froude number F_u increases above 0.1. The trend of variation of the relative energy loss $\Delta E/E_u$ for b/B =0.6 occupies an intermediate position between these two trends for contraction ratios b/B less than or equal to 0.7 or greater than or equal to 0.5. Again for the same Froude number, F_u, the relative energy loss increases rapidly as the channel contraction increases. Especially, this increase is quite significant for the channel contraction greater than 0.7. For higher Froude number above 0.2 (in the subcritical range of flow of the present investigation) this in increase is several folds compared to the minimum channel contraction b/B of 0.9.

As shown in Fig.7, for each plot, the groups of curves representing the relationship between relative upstream energy loss $\Delta E_u/E_u$ and upstream Froude number, F_u, at various contraction ratios b/B of 0.9, 0.8, 0.7, 0.6, 0.5 and 0.4 at a fixed value of angle θ for different discharges Q of 15 Lit/sec and 40 Lit/sec. It clear that, the trend of variation $\Delta E_u/E_u$ is quite similar in its behavioral characteristics to the one described above for total energy loss $\Delta E/E_u$, but with reduced magnitude, as ΔE_u constitutes a part of the total energy loss ΔE. The study of each plot show that both $\Delta E_u/E_u$ and F_u increase with the increasing value of contraction ratio b/B. The value of $\Delta E_u/E_u$ was nonlinear function of F_u. Also, it is clear that, with the same value of contraction ratio b/B, the $\Delta E_u/E_u$ increases with the increasing upstream Froude number F_u. The decrease of the channel contraction, reduces separation zone, decreasing the upstream energy loss. It can be observed that by

extending the lower sides of curves through the point F_u=0, $\Delta E_u/E_u$=0, the hydrostatic condition prevails. An extension of the upper limbs of the earlier curves, till it reaches an optimum value of contraction ratio b/B.

Fig.8 demonstrates the relationship between relative downstream energy loss $\Delta E_d/E_d$ and upstream Froude number F_u for different contraction ratios b/B of 0.9, 0.8, 0.7, 0.6, 0.5, and 0.4 at a fixed value of expansion angle θ for discharges of 15 Lit/sec and 40 Lit/sec. Again the resulting curves indicated the same trend as discussed above for ΔE and ΔE_u. It is observed that, the downstream energy loss, ΔE_d (at water structure outlet) are more than the corresponding upstream energy losses (at water structure inlet), probably due to the creation of the larger recirculating fluid mass; separated flow at the outlet of the water structure in the expansion zones. Fig.9 shows the variation relative energy (efficiency) E_d/E_u with upstream Froude number F_u for different contraction ratios b/B of 0.9, 0.8, 0.7, 0.6, 0.5 and 0.4 for discharges of 15 Lit/sec and 40 Lit/sec at a fixed values of expansion angle and bottom slope. From this figure, it can be observed that for discharge, the trend of variation between E_d/E_u and F_u is decreasing with nonlinear trend. Also, at a particular F_u, E_d/E_u increases as channel contraction decreases. It is observed that the effect of F_u on E_d/E_u is significant. The E_d/E_u increases non-linearly with the decrease of F_u. Also, the E_d/E_u increases as the discharge decreases. Fig.10 shows the variation of relation water depth Y_d/Y_u as a function of upstream Froude number F_u at different contraction ratios b/B of 0.9, 0.8, 0.7, 0.6, 0.5 and 0.4 for discharges of 15Lit/sec and 40 Lit/sec at a fixed value of bottom slope and expansion angle. It is clear that, the trend of variation Y_d/Y_u is quite similar in its behavioral characteristics to the one described above for relative energy E_d/E_u. The study of each plot shows that Y_d/Y_u increases as F_u decreases with the decreasing of channel contraction. The value of Y_d/Y_u was nonlinear function of F_u. Fig.11 depicts the variation of relative heading up $\Delta Y/Y_u$ as a function of upstream Froude number F_u for different contraction ratios b/B of 0.9, 0.8, 0.7, 0.6, 0.5 and 0.4 for discharges of 15 Lit/sec and 40 Lit/sec at a fixed values of expansion angle θ and bottom slope S_o. From this figure, it is observed that the effect of F_u and Y_d/Y_u is significant. The Y_d/Y_u increases non-linearly with the increase of F_u. Also, at a fixed discharge Q, the trend of variation between Y_d/Y_u and F_u is increasing with a nonlinear trend. Also, at a particular F_u, Y_d/Y_u increases as the channel contraction increases.

Figs.12 and 13 depict the variation of streamwise and vertical components of turbulence intensities ú/U_o and ύ /U_o as functions of channel depths y/y_o in the expansion zone of water structure at different expansion angles θ of 15°, 30°, 45° and 90° at different contraction ratios b/B of 0.7 and 0.5 for discharge of 40 Lit/sec along the depth at different cross sections. The trend of variation of ú/U_o and ύ /U_o are similar in all the cases of expansion angles. The trend of ú/U_o and ύ /U_o in the expansion zones in all the cases of expansion angles θ have higher values close to the bed, following a gradual fall in the wall region defined by $y/y_o<0.2$, reaching minima in the core region defined by $0.2<y/y_o<0.6$. Turbulence intensities ú/U_o and ύ/U_o rise gradually and then rapidly in the upper region (free surface region) defined $y/y_o>0.6$, reaching the maximum at the free surface. The minimum turbulence intensities ú/U_o and ύ /U_o always lie in the core region. The maximum turbulence intensities occur close to the bed or at the free surface depending on the location of the profile station. The nature of these variations is similar in all the cases of expansion angles, contraction ratios and discharges. Fig.13 shows the turbulence intensities ú/U_o and ύ /U_o at b/B = 0.5 of the expansion angles θ of 15°, 30, 45°, and 90°. The profiles of ú/U_o and ύ /U_o in the expansion zones of the hydraulic structures, which depict the turbulence behavior more dearly, in expansion angle θ of 90° indicate large magnitude of turbulence in the wall and free surface regions, with fairly uniform turbulence in the core region. However, for expansion angle θ=15°, turbulence profile is fairly uniform with comparatively less increase of the turbulence in wall and free surface regions. In case of expansion angle θ=90°,as shown in Fig.13, the nature of variation in turbulence intensities ú/U_o and ύ /U_o at the entry of expansion zones and subsequent sections downstream is somewhat distinct compared to the turbulence profiles in the case of gradual expansion θ=15°. Herein, in the core region of sudden expansion θ of 90°, turbulence intensity profiles ú/U_o and ύ /U_o do not exhibit the tendency towards constancy unlike in the gradual expansion, θ=15°. Generally in sudden expansion θ=90° after reaching the minimum turbulence intensities ú/U_o and ύ/U_o as the flow distance increases from the wall, the turbulence tends to increase consistently till the free surface is reached. Turbulence intensities are particularly largest ú/U_o = 45%, ύ /U_o = 29% and ú/U_o =55%, ύ/U_o=35% at x/b=2, z/b=0 and x/b=2, z/b=0.3 closer to the wall region and free surface region respectively. Similarly, both the turbulence intensities ú/U_o and ύ /U_o are large at all the sections investigated downstream of the inlet of expansion zone in 90° sudden expansion in the wall region and free surface region. The general trend in variation of depthwise turbulence is similar in the expansion zone up to x/b=6 observed in this work. Generally, the turbulence intensities ú/U_o and ύ /U_o grows rapidly after the flow separation and spreads in vertical direction in all cases of expansion angle. Also, it can be seen that the gradual expansion θ of 15°, is more effective in minimizing the turbulence intensity in the expansion zones compared to the 90° expansion angle. Downstream of the inlet of the expansion zone along the centerline, it is noted that, farthest downstream at x/b=6, turbulence intensities ú/U_o and ύ /U_o along the axis and z/b=0.3 are lowest for 15° expansion. However increase sharply at the free surface. Concluding, gradual expansion decreases the depthwise turbulence intensities ú/U_o and ύ /U_o in wall and free surface regions compared to the sudden expansion. This dampening effect could be attributed to the reduced magnitude of surface waves observed in the gradual expansion compared to relatively larger surface waves in the 90° sudden expansion. Further, the results show the influence of the expansion angle(diversion angle) on the turbulence intensities ú/U_o and ύ /U_o, which decrease with reduced diversion angle. Moreover with the increasing expansion and channel contraction, the vertical variation in turbulence intensities ú/U_o and ύ /U_o become more pronounced. Changing rapidly in the wall, core and the free surface region.

Figs.14 and 15 depict the variation of streamwise and vertical components of turbulence intensity fluctuations ú/U_o and ύ /U_o along the centerline at relative water depth y/y_o = 0.5 above the bed in the expansion zones for the flow of 40 Lit/sec, at different contraction ratios b/B of 0.5 and 0.7, at different expansion angles θ of 15°, 30°, and 90°. Clearly, the trend of turbulence intensities ú/U_o and ύ /U_o variation are quite similar in all the cases of expansion angles θ and

contraction ratio b/B. Following a slight general fall, reaching minima, turbulence rises rapidly to reach maxima with subsequent monotonous decrease along the distance away from the outlet of hydraulic structure. Generally, maximum turbulence intensities ú/U_o and ǘ /U_o occur at the same location with slight shift noticed for gradual expansion Θ=30°. The salient feature of the variation observed are as follow. For contraction ratios b/B of 0.7 and 0.5, the minimum values of ú/U_o and ǘ /U_o occurring at 0< x/b< 1.5 for all the expansion angles. The maximum values of ú/U_o and ǘ /U_o accruing at 2.2< x/b< 4.5. Similar trends are observed for turbulence intensities ú/U_o and ǘ /U_o for all contraction ratios b/B of 0.5 and 0.7 of the different expansion angles Θ of 15°, 30°, and 90°. It may be concluded that downstream of the water structures beyond specific values of x/b for instance 3.8, turbulence intensities ú/U_o and ǘ /U_o are always higher in the case of 90° sudden expansion and lower for most gradual expansion of 15°, for all contraction ratios b/B of 0.7 and 0.5. The trend is exactly opposite as observed for x/b< 2.7. Also, it may concluded that turbulence intensity beyond x/b = 4.1 from the centre of the hydraulic structure decreases with angle of diversion decreases and is subsequently higher as for sudden expansion Θ=90°, the lowest for gradual expansion Θ of 15° and being the intermediate for gradual expansion Θ=30°. The trend is reverse for x/b < 2.7where the turbulence intensity is higher for gradual expansion Θ=15° and lower for 90° sudden expansion. At x/b of 2.7 up to 4.2, the maximum turbulence intensities ú/U_o and ǘ /U_o occur for all the expansion angles at different contraction ratios b/B and all different spanwise locations. Also, with increasing channel contraction, the turbulence intensities ú/U_o and ǘ /U_o increase for all the cases.

VI. CONCLUSIONS

The conclusions arising out from this study can be summarized as follows:

Form the evidence of the variation of the total energy loss $\Delta E/E_u$ with the expansion angle in the expansion zones downstream of the water structures, it appears that up to expansion angle of 30° and decreasing the expansion angle, the head loss decreases, but above this expansion angle of 30°, the effect of the boundary is insignificant. The energy loss is quite high if the contraction ratio b/B > 0.7. The energy loss increases rapidly up to expansion angle of 30° and tends to remain constant above expansion angle of 45°. Thus, expansion angle of 30° appears to be a critical angle defining a border value between the maximum energy loss and the value up to which total energy loss increases rapidly as expansion angle increases form 0° to 30°. The results indicate that, the most significant differences in energy loss occur with expansion angle in the range less than 45°. The total energy loss $\Delta E/E_u$, upstream energy loss $\Delta E_u/E_u$, and downstream energy loss $\Delta E_d/E_d$ of the multi vents water structures, increase with the increasing value of both upstream Froude number and channel contraction. The downstream energy loss (at hydraulic structure outlet) are more than the corresponding upstream energy loss (at hydraulic structure inlet), probably due to the creation of the large recirculating fluid mass, separated flow at outlet of the hydraulic structure in the expansion zones.

The streamwise turbulence intensities ú/U_o and ǘ/U_o are higher nearer the bed in the wall region defined by $y/y_o \leq$ 0.2 due to wall effect and the free surface region defined by $y/y_o >$ 0.6 due to free surface effect. In the intermediate core region defined by $0.2 < y/y_o \leq 0.6$, minimum turbulence intensities ú/U_o and ǘ/U_o occur, and consistently correspond to the maximum streamwise mean velocity ū/U_o, occurring in the same zone approximately at the same location with the local velocity gradient being zero. In the expansion zones, gradual expansion decrease the turbulence intensities ú/U_o and ǘ /U_o in wall and free surface regions compared to the sudden expansion. The maximum values of turbulence intensities ú/U_o and ǘ /U_o occur either close to the bed or at the free surface. As a comprehensive observation, it noted that the streamwise turbulence ú/U_o is always greater compared to the vertical turbulence ǘ /U_o. Also, it is concluded that with the decreasing of expansion angle and channel contraction in the expansion zone, turbulence intensities ú/U_o and ǘ /U_o decrease at all the cases. Along the depth, the trend of variation of turbulence intensities are similar in all the expansion angles in the expansion zone of hydraulic structures, and increase or decrease simultaneously of the all cases of expansion angles.

NOMECLATURE:

ǘ Vertical component of turbulence intensity in y- direction (RMS),
x Longitudinal axis along channel length,
y Transverse axis along channel height,
z Transverse axis along channel width,
S_o Bottom slope.
Q Flow discharge
Θ Expansion angle
RMS Root mean square
b Width of hydraulic structure(total width)
B Natural channel width
ū Streamwise mean velocity in x-direction,
U_o Streamwise mean free steam, velocity averaged over the cross section.
ù Streamwise component of turbulence intensity in x-direction (RMS),
v̄ Vertical mean velocity in y-direction,

REFERENCES

[1.] Amino, R.S., and Goel, P.(1985) "Computations of Turbulent Flow Beyond Backward Facing Steps Using Reynolds Stress Closure", AIAA J., Vol. 23, No. 23, pp.1356-1361.
[2.] Chow, V.T. (1959) "Open Channel Hydraulics", Mc Graw Hill Book Co., New York, pp. 461-468.
[3.] Etheridge, D.W.,and Kemp, P.H.(1978)"Measurements of Turbulent Flow Downstream of a Rearward Facing Step", Fluid Mech. No.3.
[4.] Formica, G. (1955) "Preliminary Test on Head losser in Channels due to Cross Sectional Changes", L.Energia Electrical, Milano, Vol. 32, No.7 pp. 554-568.
[5.] Grade, H. (1993) "The Turbulent Flow Models in Open Channel Flows", Monograp, A.S. Balkema Puplishers, New Rood, V.T 08079, New Delhi, India.

[6.] Garde, R.J. (1994) "Turbulent Flow", Published by H.S. Poplai for willy Eastern limited, New Age International Limited, 4835/24, Ansari Road Daryaganj, New Delhi-110002.
[7.] Guoren, D., and Xiaonan, T. (1992) "Some Measurements of a Turbulent Structure in an Open Channel", Proceedings of the Conference of Flow Modelling and Turbulence Measurements, Ed., Zaiobao, Hemisphere Publishing Corporation, Washington.
[8.] Nakagawa, H., and Nezu, I. (1995) "Experimental Investigation on Turbulent Structure of Backward Facing Step Flow in Open Channel" J. of Hydr. Research, Vol.25, No.1.
[9.] Nezu, I., and Rodi, W., "Open Channel Flow Measurements with a Laser Doppler Velocimetry", J. Hydraulic Engg. ASCE, 112, pp. 335-355 (1986).
[10.] Nezu, I., and Nakagawa, H. (1993) "Turbulence in Open Channel Flow", IAHA-Monograph, A.A. Balkma Publishers, Old post Rood, Brookfield, VTO 5035, USA.
[11.] Nakagawa, H., and Nezu, I. (1987) "Experimental Investigation on Turbulent Structure of Back Facing step Flow in an Open Channel" J. Hydraulic Research, IAHR, 25, pp. 67-88.
[12.] Rodi, W. (1993) "Turbulence Models and their Application in Hydraulics", IAHR Monograph, A.A. Balkema Publishers, Old Post Roadfield, VTO 5036, USA.
[13.] Song, T., and Chinew, Y. (2001) "Turbulence Measurement in Nonuniform Open Channel Flow Using Acoustic Doppler Velocimeter (ADV)," J. Engg. Mech., 127 (3), 219-231.
[14.] Sukhodolov, A., and Thiele, M. (1998) "Turbulence Structure in a River Reach with Sand Beds", Water Resour., 34 (5), 1317-1334.

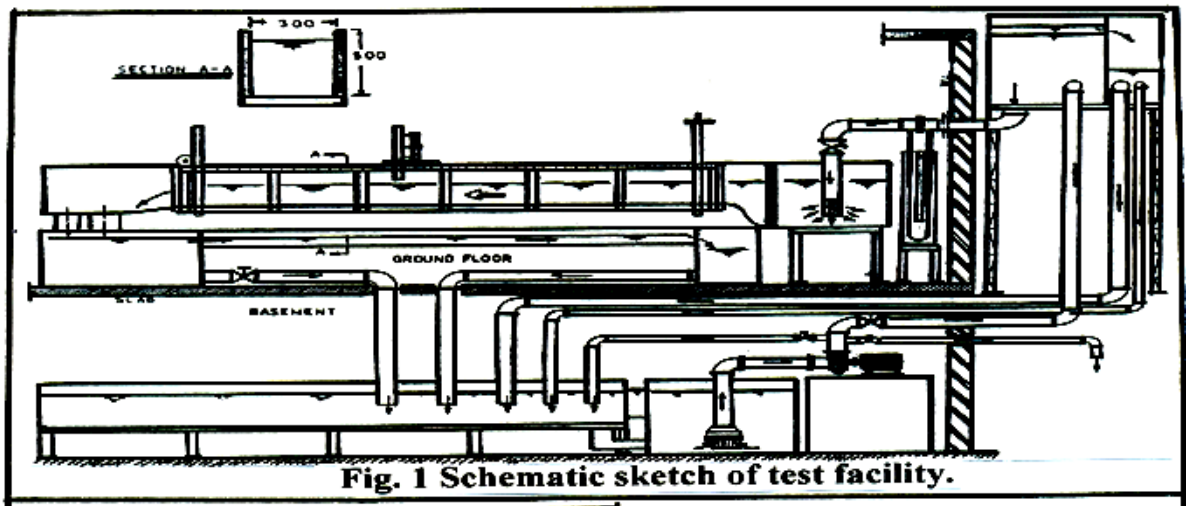

Fig. 1 Schematic sketch of test facility.

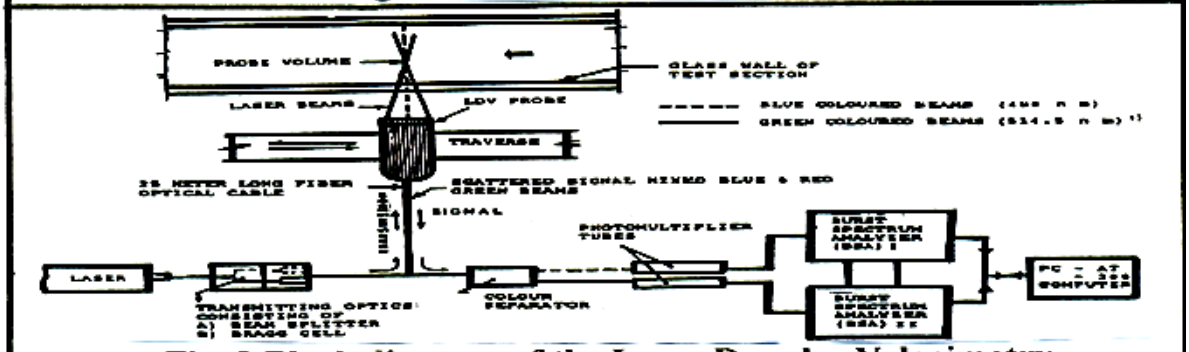

Fig. 2 Block diagram of the Laser Doppler Velocimetry.

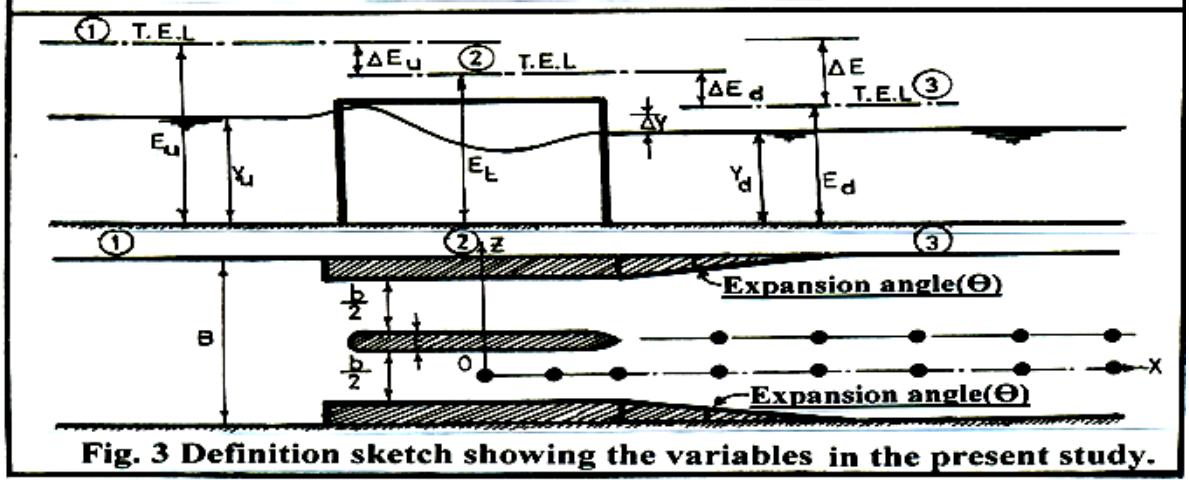

Fig. 3 Definition sketch showing the variables in the present study.

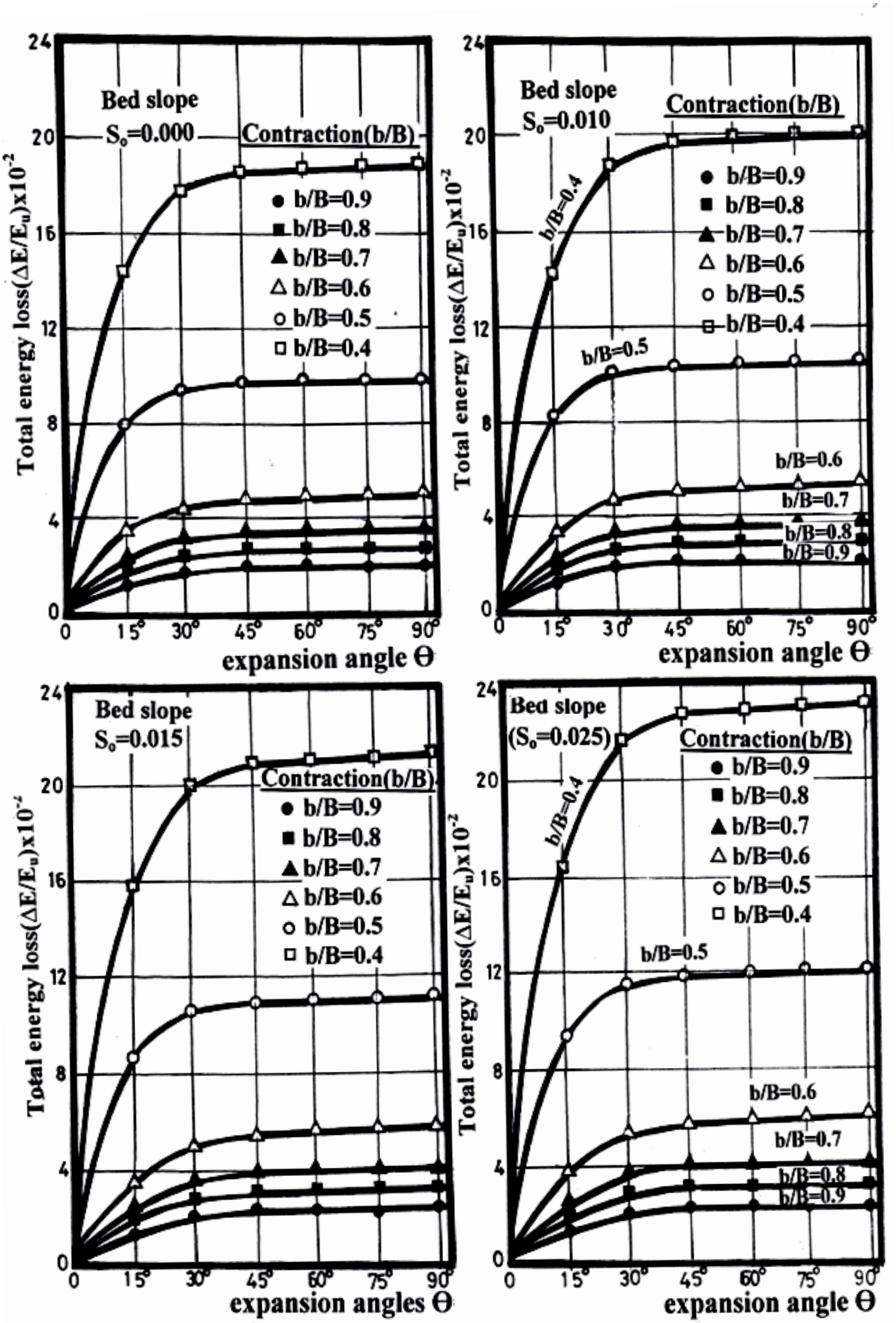

Fig.(4)Variation of total energy loss $\Delta E/E_u$ with expansion angle Θ for different contraction ratio b/B at different bottom slope S_o.

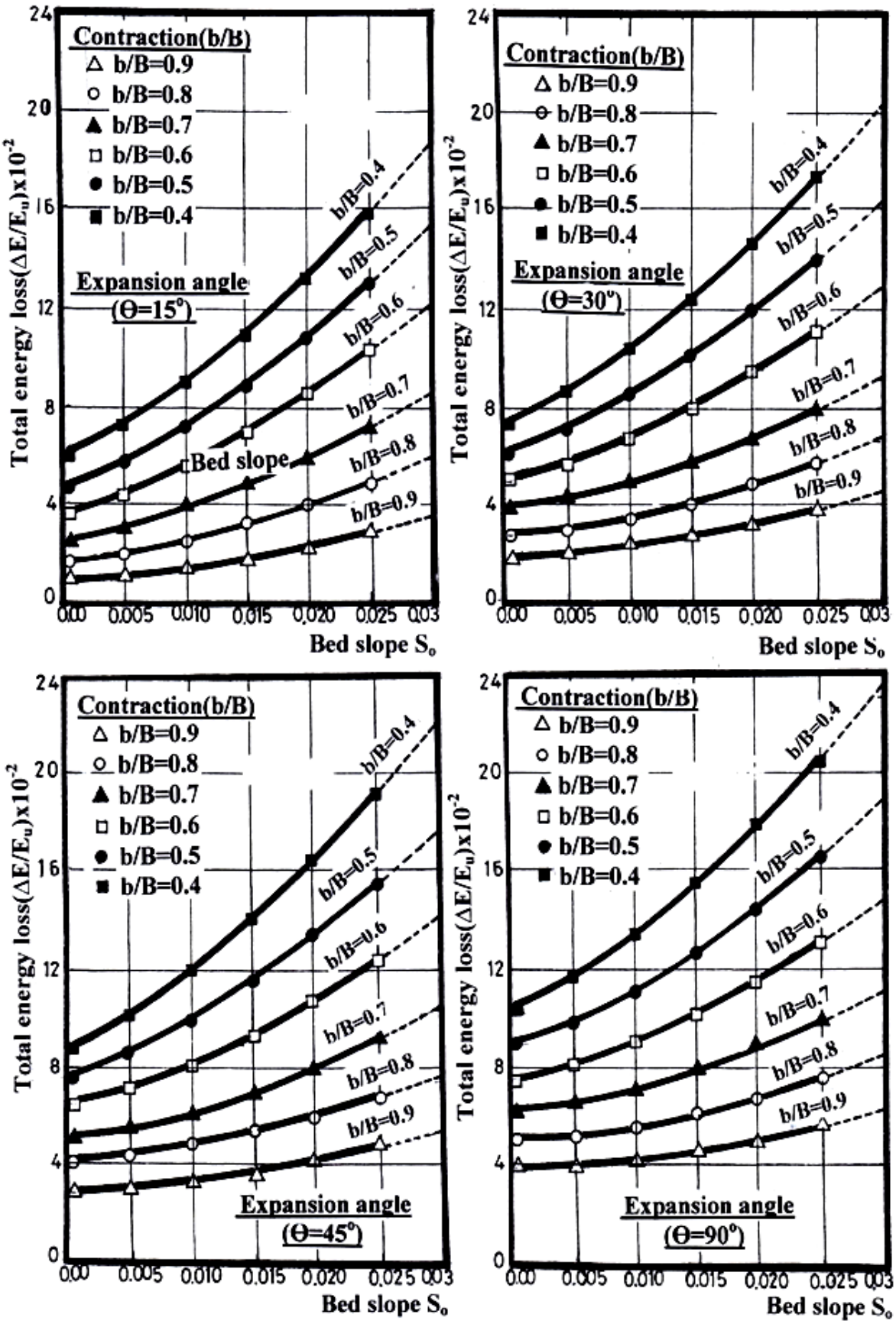

Fig.(5)Variation of total energy loss $\Delta E/E_u$ with bottom slope S_o at different contraction ratio b/B for different expansion angle Θ.

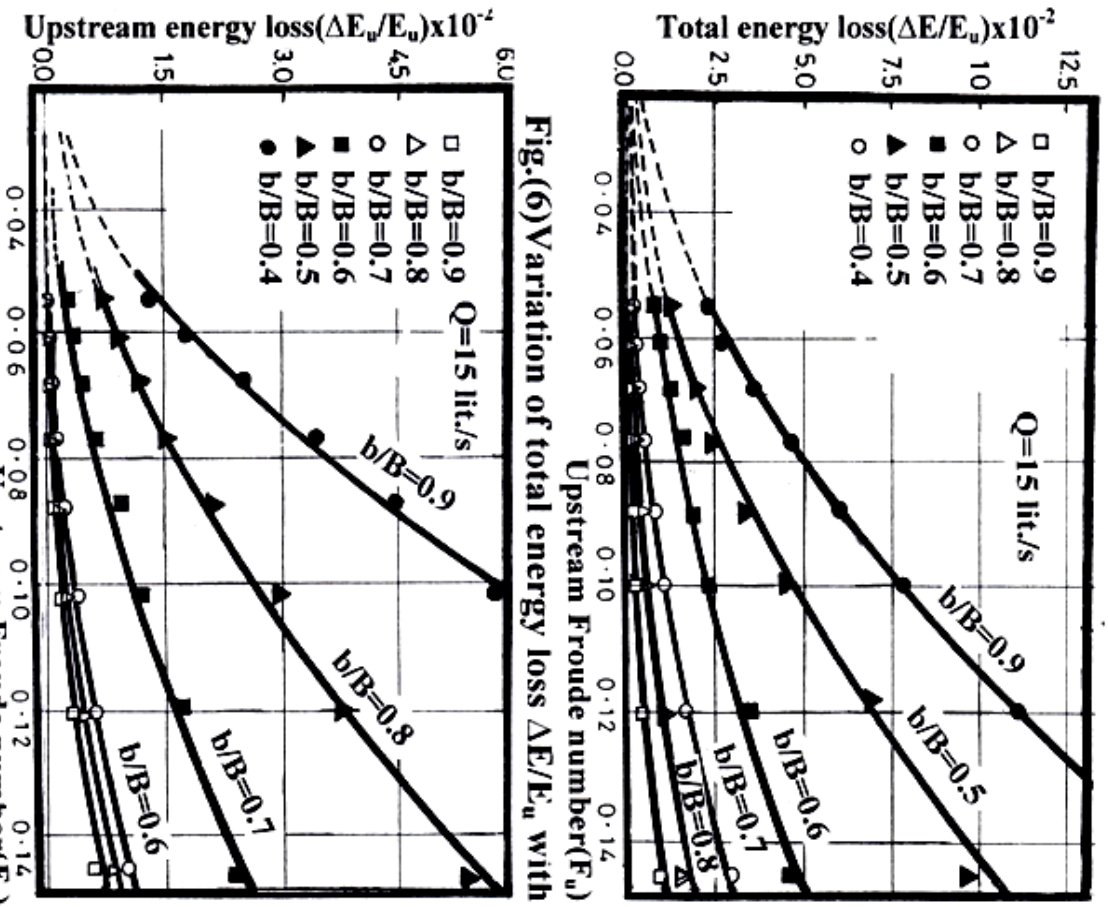

Fig.(6)Variation of total energy loss $\Delta E/E_u$ with F_u at different b/B for different discharges Q.

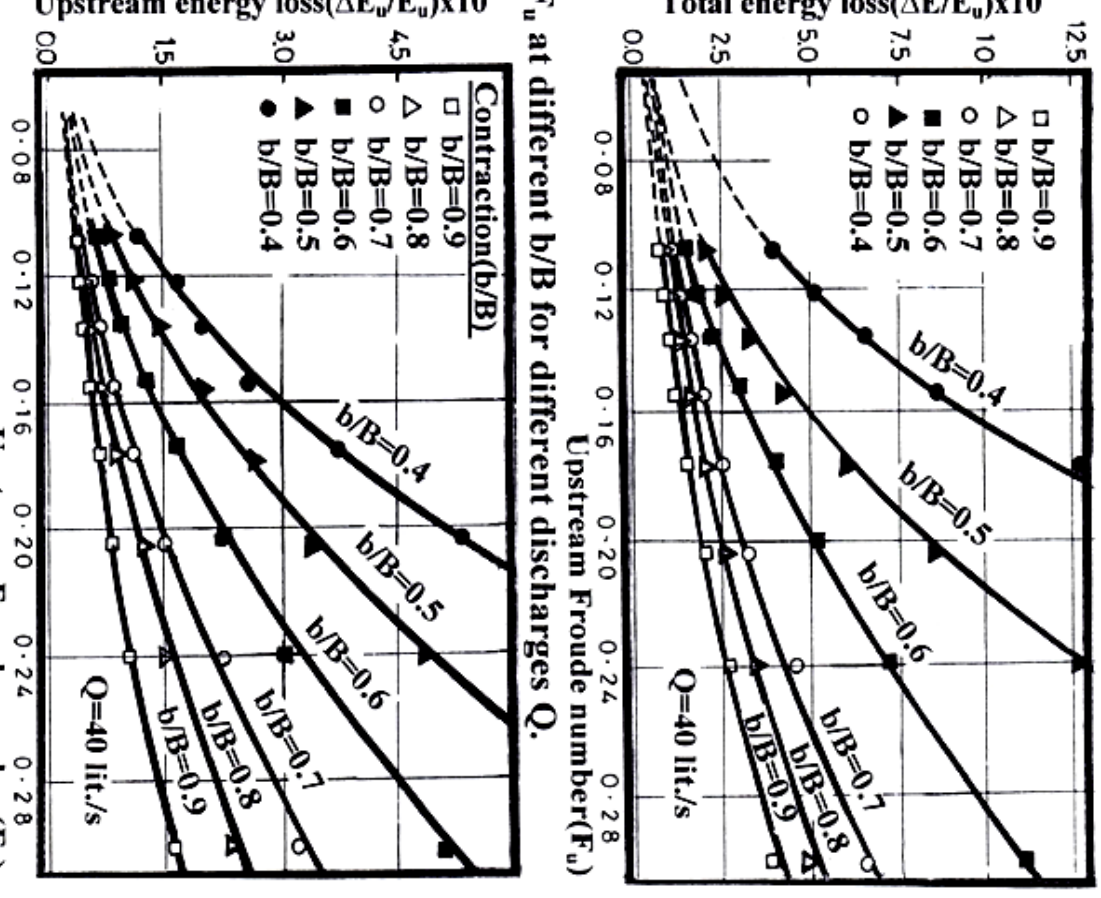

Fig.(7)Variation of upstream energy loss $\Delta E_u/E_u$ with F_u at b/B for different discharges Q.

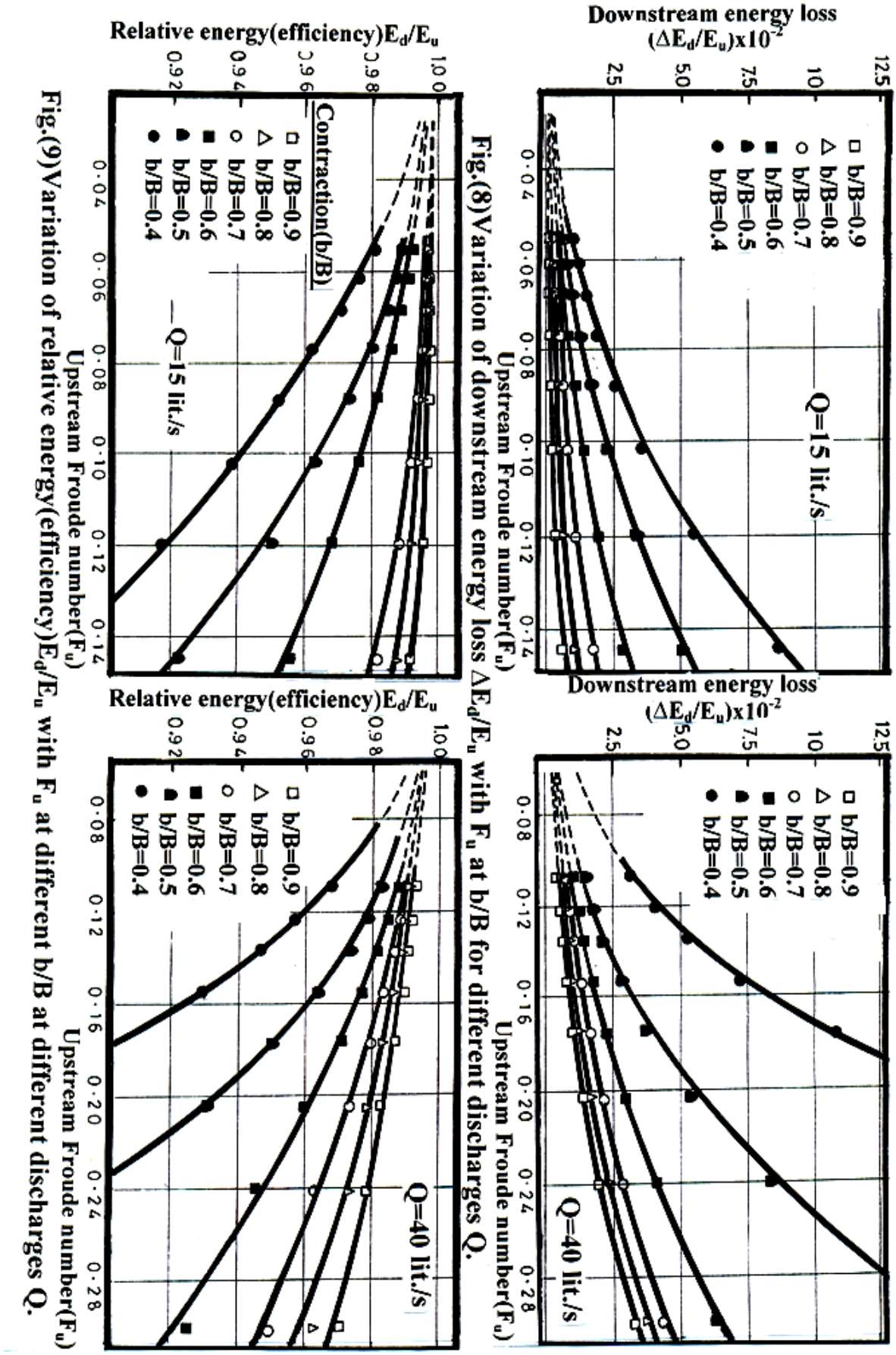

Fig.(8)Variation of downstream energy loss $\Delta E_d/E_u$ with F_u at b/B for different discharges Q.

Fig.(9)Variation of relative energy(efficiency)E_d/E_u with F_u at different b/B at different discharges Q.

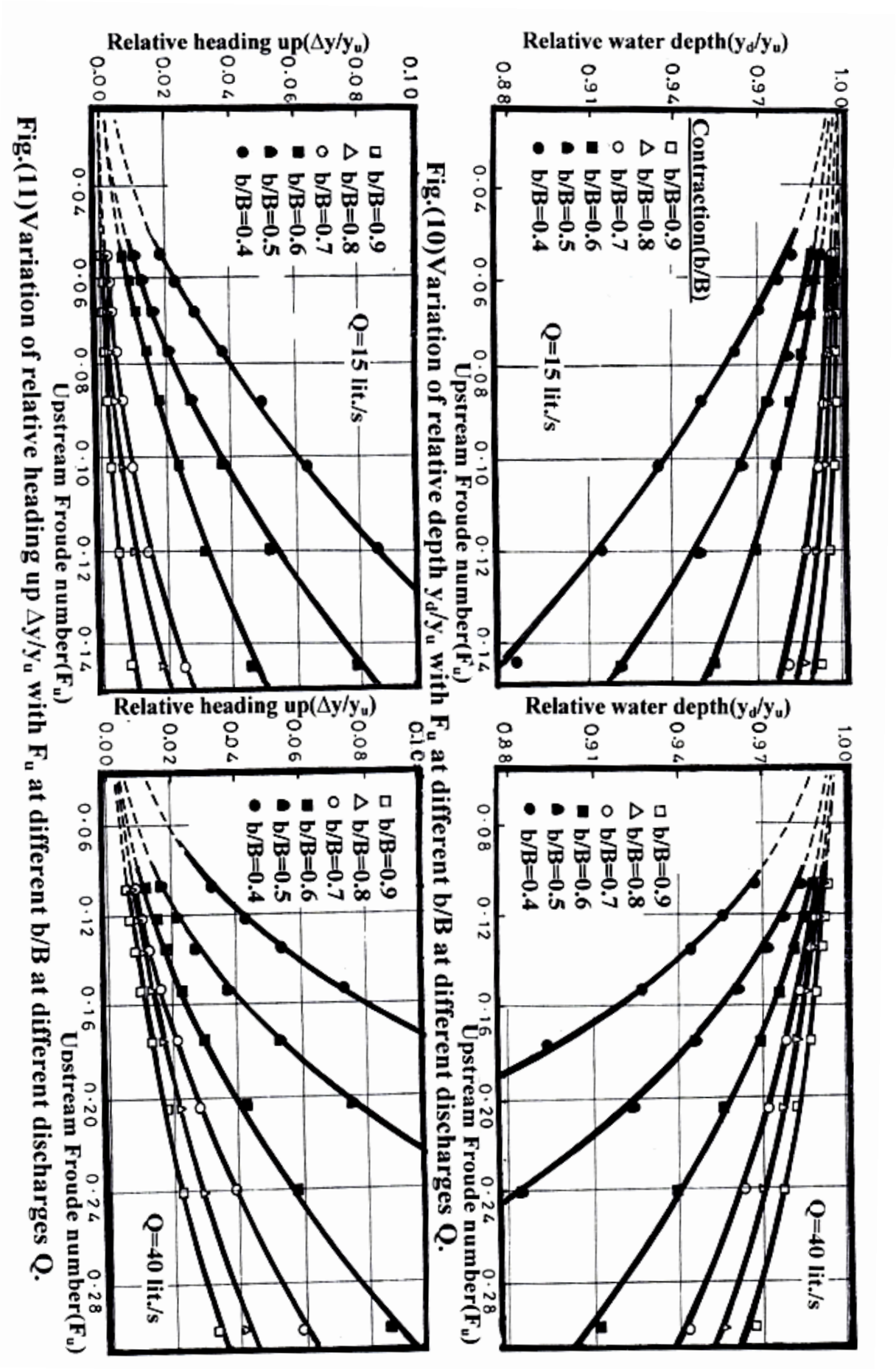

Fig.(10)Variation of relative depth y_d/y_u with F_u at different b/B at different discharges Q.

Fig.(11)Variation of relative heading up $\Delta y/y_u$ with F_u at different b/B at different discharges Q.

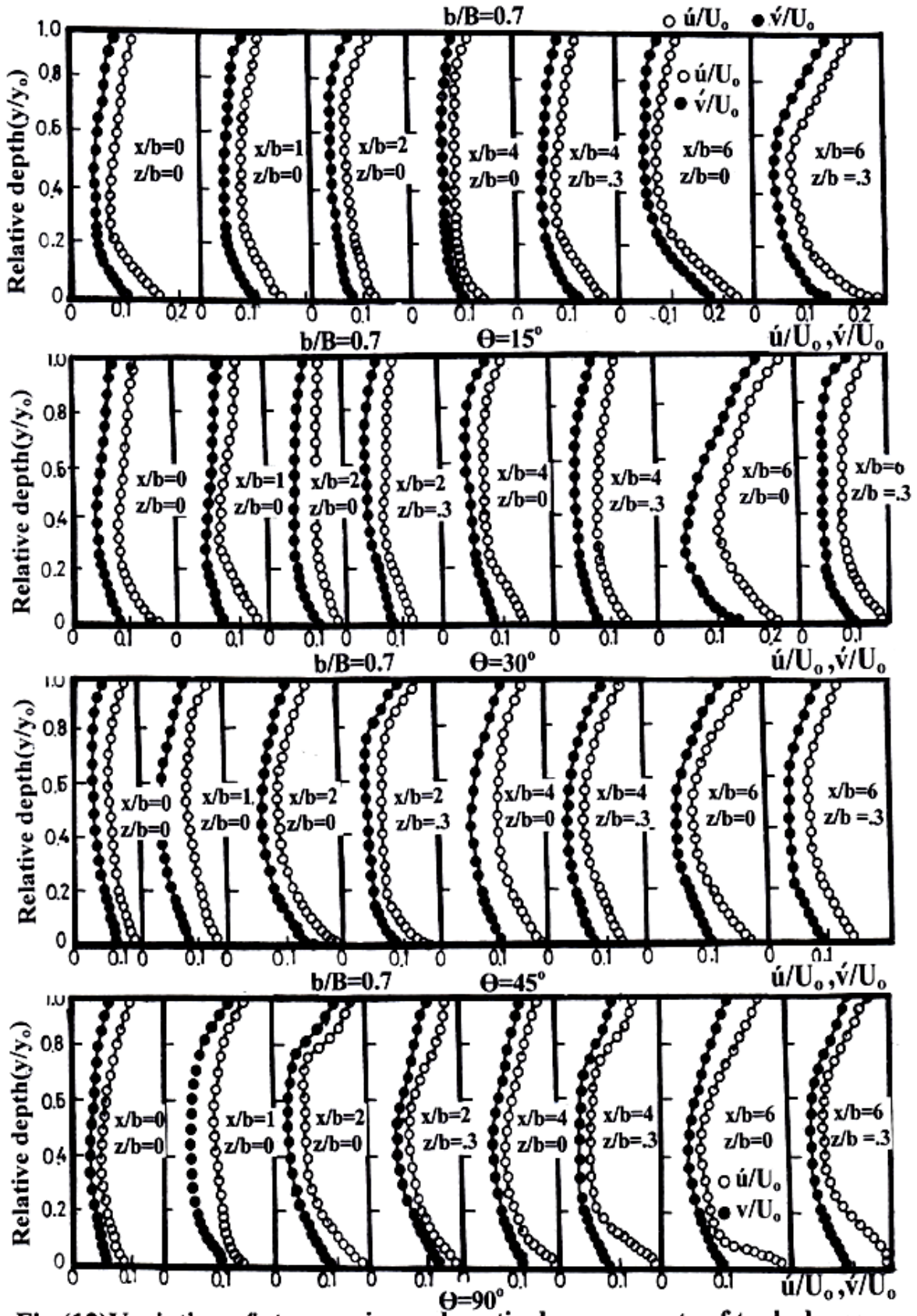

Fig.(12)Variation of streamwise and vertical components of turbulence intensities ú/U_o and v́/U_o with y/y_o in the expansion zones at b/B=0.7 at expansion angles Θ=15°, 30°,45° and90°for Q=30 lit./s .

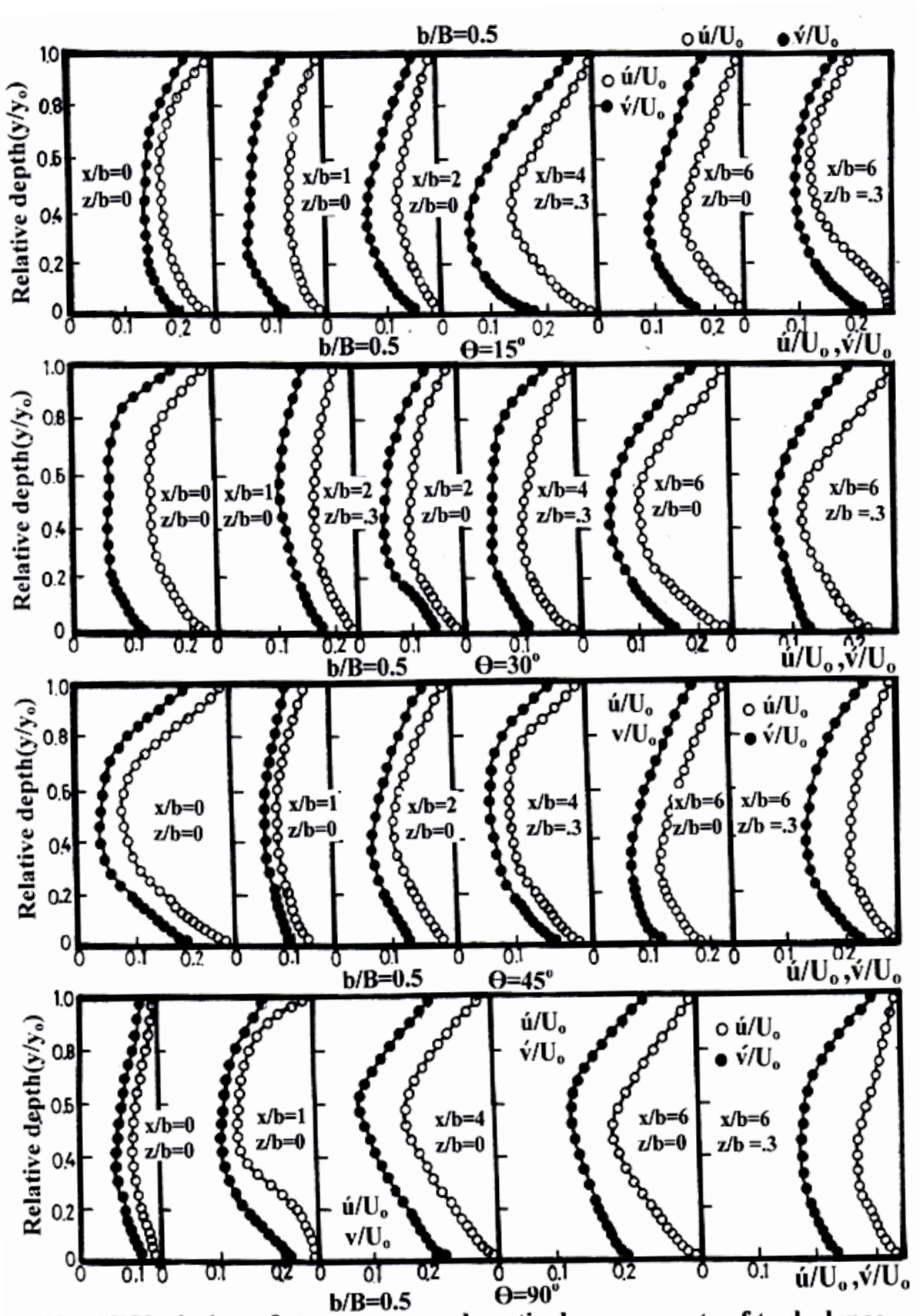

Fig.(13)Variation of streamwise and vertical components of turbulence intensities $ú/U_o$ and v/U_o with y/y_o in the expansion zones at b/B=0.5 at expansion angles $\Theta=15^o, 30^o, 45^o$ and 90^o for Q=30 lit./s .

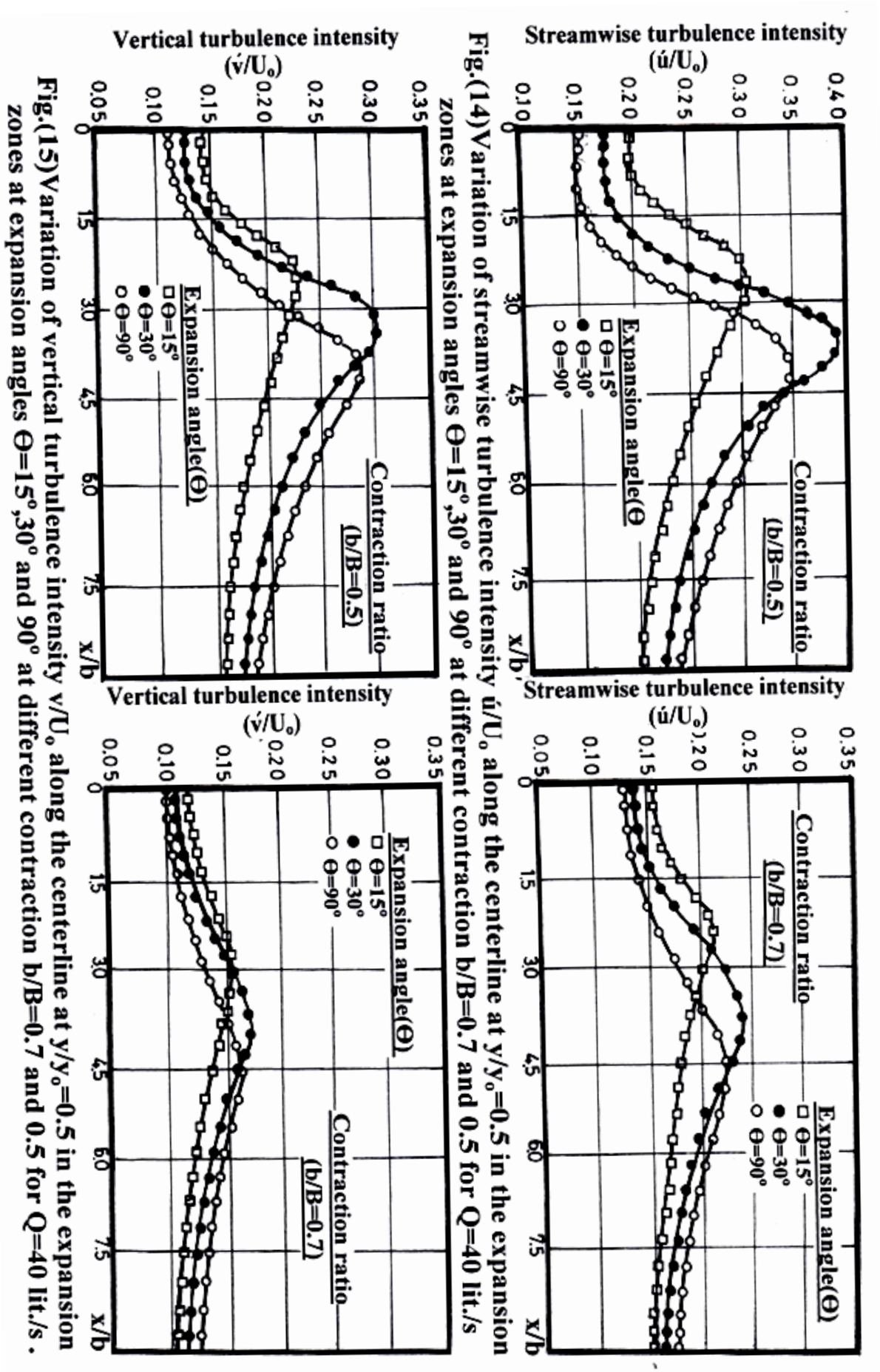

Fig.(14)Variation of streamwise turbulence intensity ú/U₀ along the centerline at y/y₀=0.5 in the expansion zones at expansion angles Θ=15°,30° and 90° at different contraction b/B=0.7 and 0.5 for Q=40 lit./s

Fig.(15)Variation of vertical turbulence intensity v/U₀ along the centerline at y/y₀=0.5 in the expansion zones at expansion angles Θ=15°,30° and 90° at different contraction b/B=0.7 and 0.5 for Q=40 lit./s .

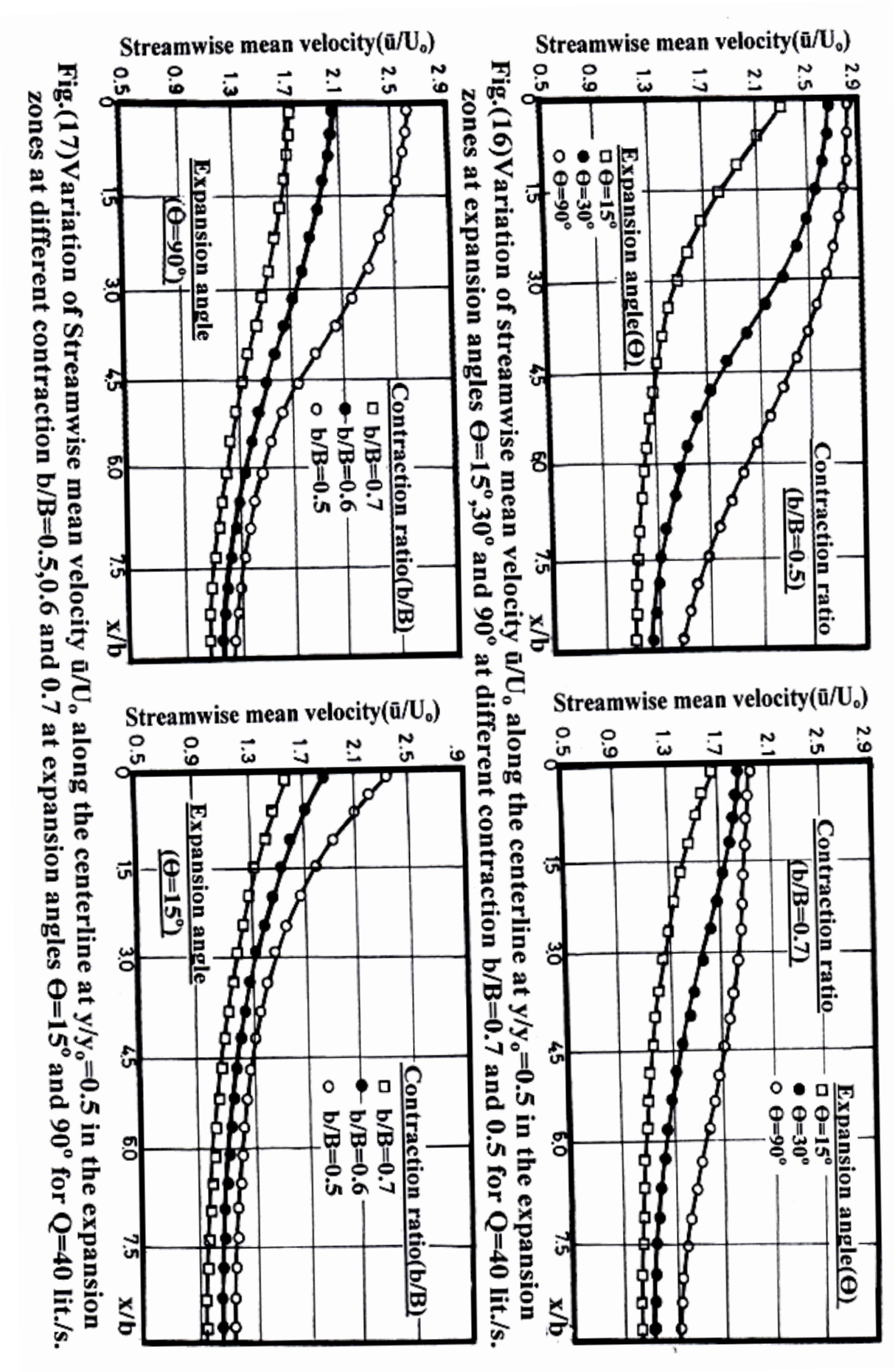

Fig.(16)Variation of streamwise mean velocity $\bar{u}/U_o$ along the centerline at y/y_o=0.5 in the expansion zones at expansion angles Θ=15°,30° and 90° at different contraction b/B=0.7 and 0.5 for Q=40 lit./s.

Fig.(17)Variation of Streamwise mean velocity $\bar{u}/U_o$ along the centerline at y/y_o=0.5 in the expansion zones at different contraction b/B=0.5,0.6 and 0.7 at expansion angles Θ=15° and 90° for Q=40 lit./s.